ACS Sustainable Chemistry & Engineering

Research Article

pubs.acs.org/journal/ascecg

Novel Lignin–Poly(*N*-methylaniline) Composite Sorbent for Silver Ion Removal and Recovery

Qiu-Feng Lü,* Jia-Jia Luo, Ting-Ting Lin, and Yi-Zhuan Zhang

College of Materials Science and Engineering, Fuzhou University, 2 Xueyuan Road, Fuzhou 350116, People's Republic of China

ABSTRACT: Lignin–poly(*N*-methylaniline) (lignin–PNMA) nanocomposites were synthesized via a chemical oxidative polymerization of *N*-methylaniline in the presence of enzymatic hydrolysis lignin (EHL). The lignin–PNMA composite consists of well size-distributed particles of 68.3 nm in mean diameter. This nanocomposite was further used as a novel sorbent for silver ions from aqueous solution. The lignin–PNMA nanocomposite particles exhibited excellent an adsorption property of silver ions compared to those of poly(*N*-methylaniline) and EHL. The saturated capacity of silver ions onto the lignin–PNMA nanocomposites was up to 1556.8 mg g^{-1} at 30 °C. Characterization results of the sorption product, i.e., lignin–PNMA nanocomposite particles after sorption, revealed that silver nanoparticles were achieved on the surface of lignin–PNMA nanocomposite particles. The results indicated that lignin–PNMA nanocomposites can be effectively used as a reactive sorbent to remove and recover silver ions from aqueous solution.

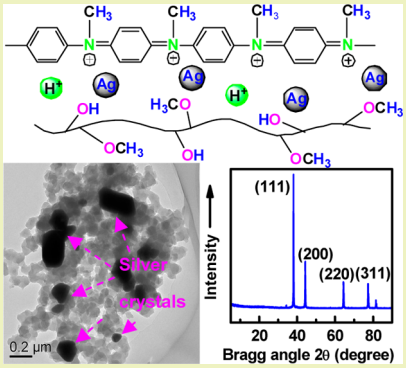

KEYWORDS: *Lignin, Poly(N-methylaniline), Silver ions, Sorption*

INTRODUCTION

Environmental pollution from industrial wastewaters containing heavy metal ions is a major worry because of the potential environmental and biological problems it may cause to humans and other life forms.[1−3] In particular, silver has been used commonly in daily life owing to its unique character and antimicrobial and antiviral properties.[4,5] Thus, effluents containing substantial silver ions have been dumped into rivers from these industries. Therefore, the removal and recovery of these silver ions from wastewaters have become important issues.[5,6] Adsorption of silver ions from effluents is considered to be a useful technique for product control of adsorbents.[7−9] Up to now, various adsorbents have been applied for removal of silver ions.[5−7] However, low-cost and effective adsorbents for silver ion removal need to be developed.

Polyaniline (PANI) derivatives have received great interest for their ease of preparation, good stability, and optimizable electrical properties. Specifically, they possess better enhanced processability than PANI.[10−13] Although a lot of research on substituted PANIs have been reported, they are mainly on ring alkyl-substituted[14,15] and ring alkoxy-substituted PANI.[16−18] Among the substituted PANIs, amino-*N*-substituted PANI derivatives, such as poly(*N*-methylaniline) (PNMA), are useful in certain applications including electrocatalytic electrodes,[19,20] cathode active material in rechargeable batteries,[21,22] corrosion protection,[23,24] and microwave shielding materials.[25] Recently, poly(*N*-methylaniline) nanowires[26] and three-dimensional microspheres[26] were obtained by adjusting the concentration of *N*-methylaniline monomers. Poly(*N*-methylaniline) microspheres have also been prepared via a template-free route[27] and electrochemical polymerization.[28] However, studies on physicochemical properties and applications of nanostructural PNMA and its composites remain to be exploited.

Lignin is a reproducible polymer generated from industrial or agricultural biomass wastes. Because lignin possesses a three-dimensional structure, which includes a great quantity of O-containing functional groups,[29,34] it has been widely applied to removing heavy metal ions such as Cu(II),[29,30] Co(II),[29] Cr(VI),[30,31] Cr(III),[32] and Pb(II)[33] from industrial effluents. In particular, lignin and lignin-based materials also exhibit high-performance for the regeneration of Au(III),[34−36] Pd(II),[36] and Pt(IV).[36] The utilization of lignin and its derivatives not only presents an effective method for adsorptive regeneration of these metal ions but also achieves high value-added utilization of biomass wastes.

Moreover, lignin and its derivatives can also be used as dispersants in various industrial fields.[37,38] Recently, we developed a controlled preparation of polyaniline–lignosulfonate nanocomposites,[39] poly(*N*-butylaniline)–lignosulfonate composite nanospheres,[40] and self-assembled poly(*N*-methylaniline)–lignosulfonate spheres[41] by using lignosulfonate as a dispersant. It was found that the introduction of lignosulfonate into the composites greatly affects their structure and properties. In light of polymers from aromatic amines[8,42−46] and polyaniline-based materials[5,47−51] that possess high reactive adsorption performance of heavy metal ions including Pb(II),[44−46]Ag(I),[5,8,9,42] Hg(II),[46−48] Au(III),[49] and Cr(VI),[50,51] the poly(*N*-butylaniline)–lignosulfonate composite nanospheres and self-assembled poly(*N*-methylaniline)–lignosulfo-

Received: September 23, 2013
Revised: November 29, 2013
Published: December 4, 2013

Scheme 1. Preparation Process of Lignin–PNMA Composite

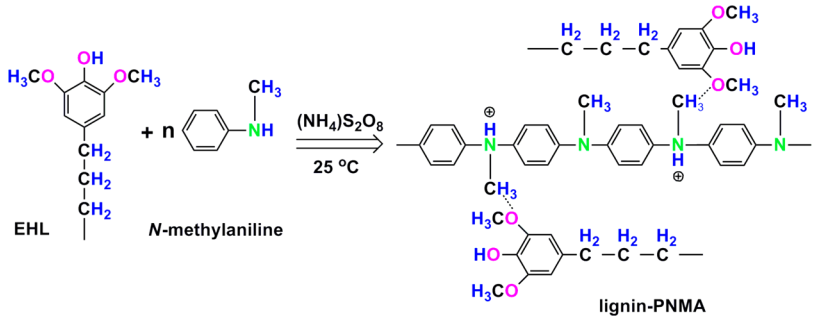

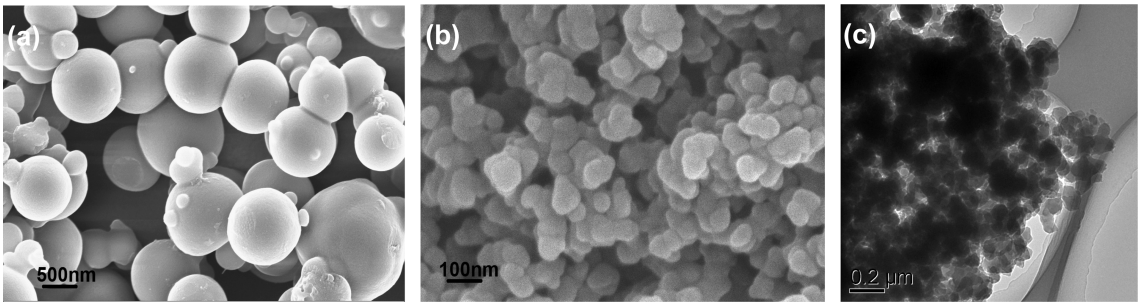

Figure 1. SEM and TEM images of PNMA (a) and lignin–PNMA composite (b,c).

nate spheres were used as adsorbents for silver ions. The results showed that they exhibited high-performance reactive adsorption for silver ions because of the introduction of lignosulfonate into the composite spheres. In addition, another novel and abundant lignin, enzymatic hydrolysis lignin (EHL),[29] was used to prepare polyaniline–lignin composites.[5] The polyaniline–lignin composite exhibited better enhanced reactive heavy metal ion adsorbability than that of polyaniline.[5,40]

The high reactive adsorbability of these composites was attributed to the existence of imino groups on polyaniline units and O-containing groups on lignin units. Synergistic effects between these functional groups endowed the composite with a high performance of heavy metal ions. For PNMA, its chemical properties are essentially different from those of PANI because the proton exchange sites on PNMA chains are irreversibly blocked by methyl substituents. Therefore, physicochemical properties of PNMA need to be studied in depth.

In this work, a new adsorbent, poly(*N*-methylaniline)–lignin (lignin–PNMA) nanocomposite particles, was prepared via a chemical oxidative polymerization of *N*-methylaniline in the existence of lignin. Furthermore, the lignin–PNMA nanocomposite particles were used to remove silver ions by using a batch adsorption technique. Adsorption kinetics and isotherms were determined by kinetic and linearized isotherm models. Specifically, the methyl groups, which have an electron-donating ability on the PNMA chains, are a benefit to increasing the adsorption properties of lignin–PNMA nanocomposites. The introduction of EHL into lignin–PNMA was responsible for the formation of low-cost nanocomposite particles.

EXPERIMENTAL SECTION

Materials. *N*-Methylaniline (NMA), ammonium peroxydisulfate, $AgNO_3$, ammonia–water, and *N*-methylpyrrolidone were obtained from Sinopharm Chemical Reagent Co. Ltd. (Shanghai, China). Enzymatic hydrolysis lignin was extracted from cornstalks and supplied by Shandong Longlive Biotechnology Co. Ltd. (Shandong, China).

Preparation of Lignin–PNMA Nanocomposites. Lignin–PNMA nanocomposites were simply prepared following our reported method,[5] with an EHL concentration of 10 wt % and a molar ratio of ammonium peroxydisulfate to NMA of 1.0 (Scheme 1). First, enzymatic hydrolysis lignin (EHL) (0.238 g) and ammonium peroxydisulfate were dissolved in a reaction medium, i.e., an aqueous solution of ammonia. Second, *N*-methylaniline (2.175 mL) was added into the EHL solution and stirred vigorously. Then, the ammonium peroxydisulfate solution was dropped into the *N*-methylaniline–lignin mixture. Lastly, the polymerization proceeded at 25 °C for 24 h. The lignin–PNMA nanocomposite was separated from the polymerization solution by filtration and thoroughly washed. The filter cake was dried at 60 °C to acquire lignin–PNMA nanocomposite powder. The pure poly(*N*-methylaniline) sample was prepared via the similar procedure above without EHL.

Silver Ion Sorption. Sorption of silver ions was performed in batch experiments.[1] Typically, the lignin–PNMA nanocomposite (30 mg) was dispersed in an $AgNO_3$ aqueous solution (15 mL). Then, the sorption solution was put in a 25 °C water bath for 48 h. After sorption, the nanocomposite was filtrated from the sorption solution. The silver ion concentration in the filtrate was determined using a Mohr method.[8,40]

Characterization. Morphologies of pure PNMA and lignin–PNMA were observed by SEM and TEM using a Carl Zeiss ULTRA 55 FESEM and JEM-2010 HRTEM, respectively. FT-IR and UV–vis spectroscopy measurements were performed on Nicolet FT-IR 5700 and Varian Cary50 Conc spectrometers, respectively. X-ray diffraction measurements were performed on a Rigaku Ultima III X-ray diffractometer using Cu Kα radiation. The thermal properties of pure PNMA and lignin–PNMA were carried out by thermogravimetric analysis (SDT-Q600, U.S.A.) in the 25–1000 °C temperature range under a nitrogen atmosphere. The pore volumes and Brunauer–Emmett–Teller (BET) surface areas were tested on a Micromeritics ASAP 2020 sorptometer by N_2 adsorption at 77 K.

RESULTS AND DISCUSSION

Morphology. The morphology of PNMA and the lignin–PNMA composite was characterized by SEM and TEM (Figure 1). The lignin–PNMA composite is composed of particles with a mean diameter of 68.3 nm in a range from 46.3 to 78.0 nm

dx.doi.org/10.1021/sc400475r | ACS Sustainable Chem. Eng. 2014, 2, 465–471

(Figure 1b), whereas the PNMA sample was composed of spheres with smooth surfaces and average diameters of 417 nm (Figure 1a). The composite particles were further confirmed by the TEM image (Figure 1c), which revealed that the lignin−PNMA composite was composed of solid nanoparticles. Clearly, there was a significant decrease in the average diameter of the lignin−PNMA composite with adding EHL. The decrease in the diameter of the composite particles was attributed to the formation of hydrogen bonds between $-OCH_3$ and −OH groups on EHL backbones and imino groups on PNMA units.[52−54] The hydrogen bond interaction is ensured by the EHL chain adsorbed on the PNMA chains during the polymerization process. EHL therefore serves as the template during the formation of the composite and further efficiently stabilizes the nanocomposite particles. Furthermore, the introduction of these oxygen-containing groups into the lignin−PNMA composite will enhance the sorption performance of the lignin−PNMA composite for heavy metal ions.

FT-IR Spectra. As shown in Figure 2, the absorption peak at 3430 cm^{-1} is attributed to an O−H stretching vibration of

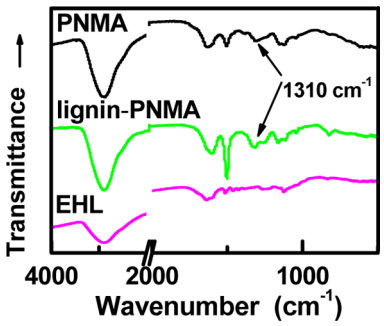

Figure 2. FT-IR spectra of PNMA, lignin−PNMA nanocomposite, and EHL.

hydroxyl groups on the EHL chain.[29] The characteristic bands at 1640, 1510, and 1460 cm^{-1} are the aromatic ring vibrations of EHL.[29] While absorption peaks at 3440−3450 cm^{-1} correspond to the N−H stretching vibration of PNMA and lignin−PNMA composites, indicating the existence of secondary amino groups in their chains.[9,42,43,45] It can also be seen that the ring stretch of the benzenoid form of the two samples was observed at about 1500 cm^{-1}. The ring stretch of the quinoid form of PNMA appeared around 1630 cm^{-1} as a notably broad band, whereas this band of the lignin−PNMA composite shifted to 1600 cm^{-1},[55] which was attributed to the interaction between the two. Bands for the C−N stretching vibration of the quinoid rings were at 1310 cm^{-1}.[27]

UV−Vis Spectra. As displayed in Figure 3, for the EHL sample, one characteristic peak at 310 nm was observed, which was attributed to the α,β-unsaturated and/or α-carbonyl groups.[56] In the UV−vis spectra of PNMA and lignin−PNMA, peaks of the $\pi-\pi^*$ transitions in the benzenoid structure were at 322 nm.[46,57] In the spectra of PNMA, the peak at 581 nm was ascribed to the $n-\pi^*$ transitions in quinoid.[27,46,57] For the lignin−PNMA nanocomposite, however, the $n-\pi^*$ band exhibited a red-shift to 623 nm, indicating an increased extent of conjugation. The reason for this might be due to a doped effect of EHL into the PNMA chains. This result agreed with the FT-IR result, which suggested that a close combination was formed between the EHL and PNMA chains.

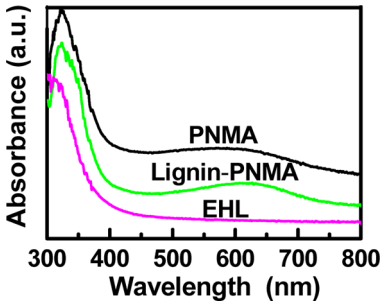

Figure 3. UV−vis spectra of PNMA, lignin−PNMA nanocomposite, and EHL.

Thermogravimetric Analysis. As shown in Figure 4, compared with PNMA and EHL, the lignin−PNMA nano-

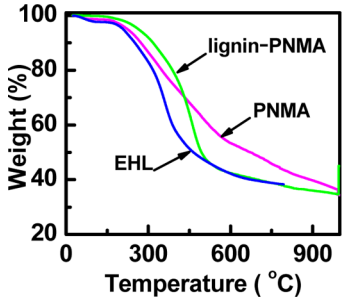

Figure 4. TGA curves of PNMA, lignin−PNMA nanocomposite, and EHL.

composite exhibited higher thermal stability. The nanocomposite exhibited a first weight loss of 1.62% before 200 °C for the evaporation of water in the sample.[9] The second weight loss at 200−500 °C mainly resulted from the thermal elimination of the alkyl and alkoxy side groups.[9,58] The weight loss of the lignin−PNMA nanocomposite occurred between 500 and 600 °C because of the breakdown of lignin−PNMA backbone. The pyrolytic process became gentle at temperatures higher than 600 °C. The higher thermal stability of the nanocomposite was probably due to the existence of an interaction between the two components. Furthermore, compared with the polyaniline−lignin composite,[5] lignin−PNMA possessed higher thermal stability. This is because the oxidative degradation of imino groups on the lignin−PNMA nanocomposite was reduced.[59]

Sorption of Silver Ion. The variation of sorption performance of silver ions onto lignin−PNMA, PNMA, and EHL is listed in Table 1. The adsorption capacity (Q_e) andadsorptivity (q) of lignin−PNMA nanocomposites were up to 1215.0 mg g^{-1} and 45.0%, respectively, when initial silver ion concentration was 50 mmol L^{-1} at 30 °C for 48 h. Clearly, the lignin−PNMA exhibits higher sorption performance than PNMA and EHL. This enhanced adsorption capacity and adsorptivity of lignin−PNMA nanocomposites resulted from

Table 1. Variation of Sorption Performance of Silver Ions on PNMA, Lignin−PNMA, and EHL

sample	Q_e (mg g^{-1})	q (%)
PNMA	548.6	20.3
lignin−PNMA	1215.0	45.0
EHL	631.3	23.4

dx.doi.org/10.1021/sc400475r | ACS Sustainable Chem. Eng. 2014, 2, 465−471

the synergistic effect between the functional groups from PNMA and EHL.[5]

Effect of Initial Solution pH Value. As illustrated in Figure 5, the initial solution pH value greatly affects the silver ions sorption on the lignin−PNMA nanocomposite. The adsorption capacity and adsorptivity exhibit significant increases in the silver ions sorption when the initial pH value increased from 1.0 to 6.0. The adsorption capacity gradually enhanced within the pH range of 1.0−5.65 and reached a maximum value at 6.0. At lower pH, the adsorption capacity and adsorptivity for silver ions is low. This is because an excess proton in the sorption solution can compete with silver ions for the available exchange sites.[60] At the same time, the hydroxyl and imino groups on the lignin−PNMA nanocomposite were protonated, i.e., the adsorbent surface carry more positive charges at lower pH values. With increasing the initial pH value from 1.0 to 5.65, imino and hydroxyl groups were gradually deprotonated; and hence, the silver ions sorption capacity was greatly enhanced.[42] However, silver ions will precipitate when the pH value is higher than 5.65. Therefore, the adsorption capacity and adsorptivity for silver ions at a pH value of 6.0 resulted from the precipitate of silver ions from the adsorption solution. This result is different from the sorption of silver ions on poly(o-phenylenediamine)[42] and poly(1,8-diaminonaphthalene) microparticles.[8] Thus, an initial pH value of 5.65 is optimal for silver ions sorption, and it is fixed at 5.65 for the following study.

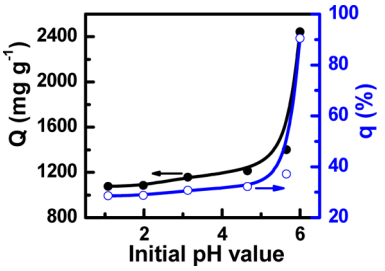

Figure 5. Effect of initial pH value on sorption of lignin−PNMA nanocomposites at a silver ion concentration of 50 mmol L^{-1} at 30 °C for 48 h.

Effect of Sorption Time. The effect of sorption time on the sorption of silver ions on lignin−PNMA is shown in Figure 6. Clearly, the sorption ability greatly increased with sorption time. The adsorption capacity and adsorptivity greatly enhanced at first and then gradually slowed to equilibrium.[8,42,45] The silver ion adsorption capacity reached 1220.1 mg g^{-1} when the sorption time was up to 72 h. Apparently, the lignin−PNMA nanocomposite has higher sorption ability than the polyaniline−lignin composite.[5] The high-performance of lignin−PNMA for silver ions is due to the synergistic effect between the functional groups.

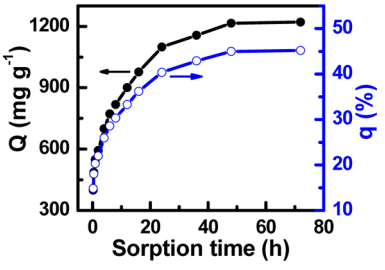

Figure 6. Effect of sorption time on sorption of lignin−PNMA nanocomposites.

Moreover, the lignin−PNMA nanocomposite has a higher Bruauer−Emmett−Teller surface area (32.65 m^2 g^{-1}) than the polyaniline−lignin composite (13.66 m^2 g^{-1}) because the former is made up of nanoparticles. The smaller diameter and higher surface area can improve the metal ion adsorbility of the lignin−PNMA nanocomposite.

Effect of Initial Silver Ion Concentration. The adsorption capacity increased while adsorptivity decreased as the initial silver ion concentration increased (Figure 7). Similar results were reported for silver ions sorption on poly(*N*-butylaniline)−lignosulfonate composite nanospheres[40] and poly(1,8-diaminonaphthalene).[8] The saturated capacity is up to 1556.8 mg g^{-1} at a silver ion concentration of 0.16 mol L^{-1}. Furthermore, the saturated capacity is higher than that of polyaniline−lignin composite.[5] The reason is that the methyl groups on PNMA have an electron-donating ability. They can strengthen the activity of *N* atoms, although the increase is a small steric hindrance. Hence, the lignin−PNMA nanocomposite exhibits higher sorption properties for silver ions.

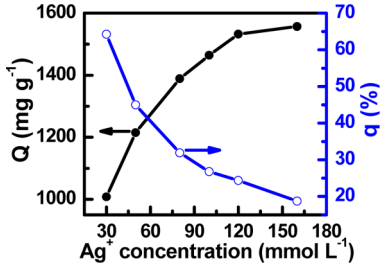

Figure 7. Effect of initial silver ion concentration on sorption of lignin−PNMA nanocomposites at 30 °C for 48 h.

Sorption Kinetics and Isotherm. From the analysis results of kinetics models[29,40,42] (Table 2), we can see that this sorption process agreed better with the pseudo-second-order model (R^2 = 0.9950) than the pseudo-first-order model. Because the former was based on a chemical sorption process, the sorption process in this work was chemical sorption.[48]

Table 2. Kinetic Parameters for Silver Ion Sorption on Lignin−PNMA

pseudo-first-order model		pseudo-second-order model	
Q_e (mg g^{-1})	730.4	Q_e (g g^{-1})	1.2322
k_1 (h^{-1})	0.07009	k_2 (g g^{-1} h^{-1})	0.07182
R^2	0.9616	R^2	0.9950

The silver ion sorption process was further analyzed by using Langmuir and Freundlich models[8,48] (Table 3). Obviously, the correlation coefficient (R^2 = 0.9986) of the Langmuir model is higher than that of the Freundlich model (R^2 = 0.9841). So, the

Table 3. Isothermal Models for the Silver Ion Sorption on Lignin−PNMA

Langmuir isotherm model		Freundlich isotherm model	
Q_m (g g^{-1})	1.6603	$1/n$	0.1828
K_L (mL mg^{-1})	1.0343	K_F (mg g^{-1})(L mg^{-1} $^{1/n}$]	280.59
R^2	0.9986	R^2	0.9841

dx.doi.org/10.1021/sc400475r | ACS Sustainable Chem. Eng. 2014, 2, 465−471

Langmuir model is a good fit for silver ions onto the lignin–PNMA nanocomposite.[8,40,48] The theoretical saturated capacity (Q_m) obtained from the Langmuir model was 1.8011 g g^{-1}, agreeing with experimental saturated capacity.

Sorption Mechanism. The sorption mechanism was further revealed by measuring the pH value variation of the silver ion solution with sorption time and TEM image of the sorption product (Figure 8). As shown in Figure 8a, the pH value declined sharply from 4.85 to 2.33 at the first 1 h, and then declined gradually, and finally reached a plateau value of 1.79. This is because the hydrogen ions on the PNMA chains were replaced by silver ions and then discharged into the sorption solution.[5,40,48,57] With prolonging the sorption time, an increase in the number of hydrogen ions led to a drop in the pH value. In the typical TEM image (Figure 8b) of the lignin–PNMA nanocomposite after silver ion sorption, a product containing silver nanoparticles was obtained. This result shows that the lignin–PNMA nanocomposite possessed high reductibility for the silver ions.[5,9,40,57] Silver ions were reduced to initial silver nanoparticles during the sorption process, and then, these initial silver nanoparticles grew into larger silver nanoparticles (Scheme 2).

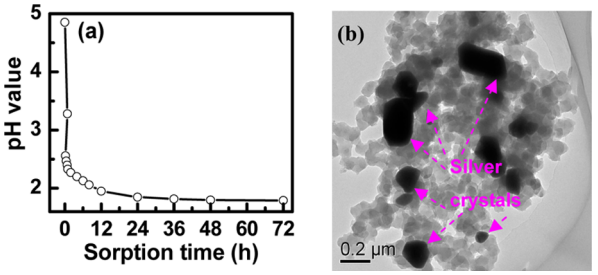

Figure 8. (a) Variation of pH value with sorption time. (b) TEM image of the sorption product.

To further prove the generation of silver nanoparticles, X-ray diffraction curves of lignin–PNMA after silver ion sorption, PNMA, lignin–PNMA, and EHL samples were characterized (Figure 9). Clearly, PNMA, lignin–PNMA nanocomposites, and EHL samples had amorphous structures[42,45,46] (Figure 9b). Compared with amorphous lignin–PNMA nanocomposites, lignin–PNMA nanocomposites after silver ion sorption, i.e., lignin–PNMA–Ag complex, have four sharp diffraction peaks at 38.08°, 44.27°, 64.42°, and 77.60°, exactly belonging to the crystal planes of silver, (Figure 9a).[5,42,57] It is concluded that silver ions can be successfully removed and recovered by using the lignin–PNMA nanocomposite as an adsorbent. Thus, the silver ions after sorption cannot be desorped from the lignin–PNMA nanocomposite surface. However, because both the silver nanoparticles[41,61] and lignin[62,63] exhibit antibacterial activities, the lignin–PNMA nanocomposite containing recovered silver nanocrystals, i.e., a lignin–PNMA–Ag complex, can be directly used as an antimicrobial.

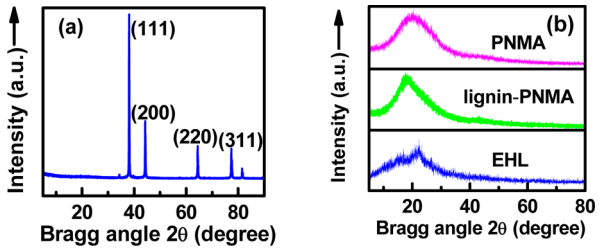

Figure 9. (a) X-ray diffraction curves of lignin–PNMA after sorption and (b) PNMA, lignin–PNMA, and EHL.

CONCLUSIONS

Lignin–PNMA nanocomposites were successfully prepared from *N*-methylaniline with enzymatic hydrolysis lignin as a dispersant. The lignin–PNMA composite consisted of well size-distributed particles with a mean diameter of 68.3 nm. Introducing EHL into the poly(*N*-methylaniline) chains can greatly affect the morphology, structure, and thermal property of the lignin–PNMA nanocomposite. The lignin–PNMA nanocomposite exhibited better thermal stability than poly(*N*-methylaniline) and EHL because of the introduction of EHL. Furthermore, the lignin–PNMA nanocomposite particles possessed excellent silver ion reactive sorption ability. The saturated adsorption capacity of silver ions onto the lignin–PNMA nanocomposite was up to 1556.8 mg g^{-1} at 30 °C. Furthermore, silver nanoparticles were recovered via a redox reaction between lignin–PNMA and silver ions. This result of this study provides a facile preparation of lignin–PNMA nanocomposites and their application to removing silver ions from wastewaters. Because EHL is a renewable material, this low-cost lignin–PNMA nanocomposite exhibits great potential to treat wastewater containing toxic heavy metal ions.

Scheme 2. Possible Sorption Mechanism of Silver Ions on Lignin–PNMA

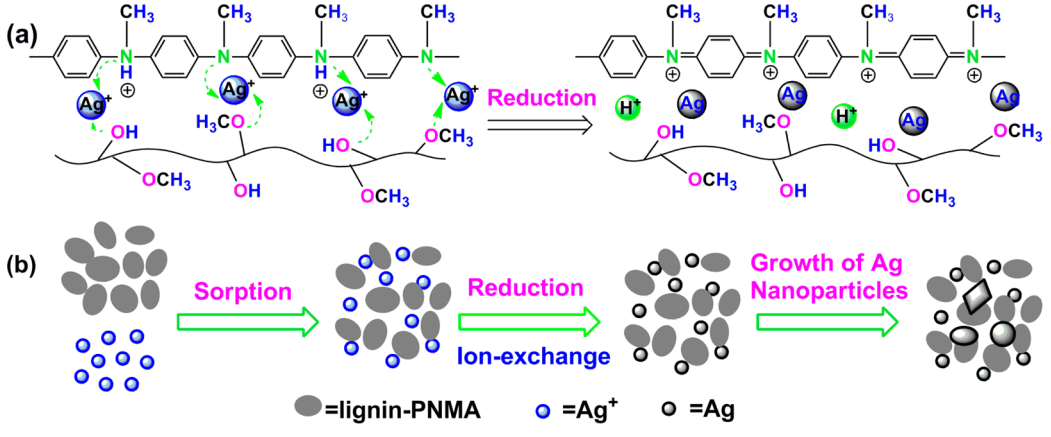

dx.doi.org/10.1021/sc400475r | ACS Sustainable Chem. Eng. 2014, 2, 465–471

AUTHOR INFORMATION

Corresponding Author

*E-mail: qiufenglv@163.com; qiufenglvfzu@gmail.com.

Notes

The authors declare no competing financial interest.

ACKNOWLEDGMENTS

This work was supported by the Natural Science Fund of Fujian Province, China (Grant No. 2012J01201).

REFERENCES

(1) Meng, Q.; Zhang, X.; He, C.; He, G.; Zhou, P.; Duan, C. Multifunctional mesoporous silica material used for detection and adsorption of Cu^{2+} in aqueous solution and biological applications in vitro and in vivo. *Adv. Funct. Mater.* **2010**, *20*, 1903−1909.

(2) Huang, M. R.; Li, S.; Li, X. G. Longan shell as novel biomacromolecular sorbent for highly selective removal of lead and mercury ions. *J. Phys. Chem. B* **2010**, *114*, 3534−3542.

(3) Bailey, S. E.; Olin, T. J.; Bricka, R. M.; Adrian, D. D. A review of potentially low-cost sorbents for heavy metals. *Water Res.* **1999**, *33*, 2469−2479.

(4) Ghassabzadeh, H.; Mohadespour, A.; Torab-Mostaedi, M.; Zaheri, P.; Maragheh, M. G.; Taheri, H. Adsorption of Ag, Cu and Hg from aqueous solutions using expanded perlite. *J. Hazard. Mater.* **2010**, *177*, 950−955.

(5) He, Z.-W.; Lü, Q.-F.; Zhang, J.-Y. Facile preparation of hierarchical polyaniline−lignin composite with a reactive silver-ion adsorbability. *ACS Appl. Mater. Interfaces* **2012**, *4*, 369−374.

(6) Wang, L.; Xing, R.; Liu, S.; Yu, H.; Qin, Y.; Li, K.; Feng, J.; Li, R.; Li, P. Recovery of silver (I) using a thiourea-modified chitosan resin. *J. Hazard. Mater.* **2010**, *180*, 577−582.

(7) Akthar, M. N.; Sastry, K. S.; Mohan, P. M. Biosorption of silver ions by processed *Aspergillus niger* biomass. *Biotechnol. Lett.* **1995**, *17*, 551−556.

(8) Li, X.-G.; Huang, M.-R.; Li, S.-X. Facile synthesis of poly(1,8-diaminonaphthalene) microparticles with a very high silver-ion adsorbability by a chemical oxidative polymerization. *Acta Mater.* **2004**, *52*, 5363−5374.

(9) Li, X.-G.; Feng, H.; Huang, M.-R. Redox sorption and recovery of silver ions as silver nanocrystals on poly(aniline-*co*-5-sulfo-2-anisidine) nanosorbents. *Chem. -Eur. J.* **2010**, *16*, 10113−10123.

(10) Chevalier, J. W.; Bergeron, J. Y.; Dao, L. H. Synthesis, characterization, and properties of poly (*N*-alkylanilines). *Macromolecules* **1992**, *25*, 3325−3331.

(11) Zotti, G.; Comisso, N.; D'Aprano, G.; Leclerc, M. Electrochemical deposition and characterization of poly(2,5-dimethoxyaniline): A new highly conducting polyaniline with enhanced solubility, stability and electrochromic properties. *Adv. Mater.* **1992**, *4*, 749−752.

(12) Gazotti, W. A., Jr.; De Paoli, M. A. High yield preparation of a soluble polyaniline derivative. *Synth. Met.* **1996**, *80*, 263−269.

(13) Li, X.-G.; Zhou, H.-J.; Huang, M.-R. Synthesis and properties of processable conducting copolymers from *N*-ethylaniline with aniline. *J. Polym. Sci., Part A: Polym. Chem.* **2004**, *42*, 6109−6124.

(14) Wei, Y.; Focke, W. W.; Wnek, G. E.; Ray, A.; MacDiarmid, A. G. Synthesis and electrochemistry of alkyl ring-substituted polyanilines. *J. Phys. Chem.* **1989**, *93*, 495−499.

(15) Wei, Y.; Hariharan, R.; Patel, S. A. Chemical and electrochemical copolymerization of aniline with alkyl ring-substituted anilines. *Macromolecules* **1990**, *23*, 758−764.

(16) D'Aprano, G.; Leclerc, M.; Zotti, G.; Schiavon, G. Synthesis and characterization of polyaniline derivatives: poly(2-alkoxyanilines) and poly(2,5-dialkoxyanilines). *Chem. Mater.* **1995**, *7*, 33−42.

(17) D'Aprano, G.; Leclerc, M. Steric, electronic effects in methyl and methoxy substituted polyanilines. *J. Electroanal. Chem.* **1993**, *351*, 145−158.

(18) Gazotti, W. A., Jr.; Matencio, T.; De Paoli, M.-A. Electrochemical impedance spectroscopy studies for chemically prepared poly(o-methoxyaniline) doped with functionalized acids. *Electrochim. Acta* **1997**, *43*, 457−464.

(19) Raoof, J.-B.; Omrani, A.; Ojani, R.; Monfared, F. Poly(*N*-methylaniline)/nickel modified carbon paste electrode as an efficient and cheep electrode for electrocatalytic oxidation of formaldehyde in alkaline medium. *J. Electroanal. Chem.* **2009**, *633*, 153−158.

(20) Yano, J.; Kokura, M.; Ogura, K. Electrocatalytic behaviour of a poly(*N*-methylaniline) filmed electrode to hydroquinone. *J. Appl. Electrochem.* **1994**, *24*, 1164−1169.

(21) Sivakumar, R.; Saraswathi, R. Characterization of poly(*N*-methylaniline) as a cathode active material in aqueous rechargeable batteries. *J. Power Sources* **2002**, *104*, 226−233.

(22) Sivakkumar, S. R.; Saraswathi, R. Performance evaluation of poly(*N*-methylaniline) and polyisothianaphthene in charge-storage devices. *J. Power Sources* **2004**, *137*, 322−328.

(23) Narayanasamy, B.; Rajendran, S. Electropolymerized bilayer coatings of polyaniline and poly(*N*-methylaniline) on mild steel and their corrosion protection performance. *Prog. Org. Coat.* **2010**, *67*, 246−254.

(24) Yağan, A.; Pekmez, N.Ö.; Yildiz, A. Electropolymerization of poly(*N*-methylaniline) on mild steel: Synthesis, characterization and corrosion protection. *J. Electroanal. Chem.* **2005**, *578*, 231−238.

(25) Li, L.; Qiu, H.; Qian, H.; Hao, B.; Liang, X. Controlled synthesis of the poly(*N*-methylaniline) Zn0.6Mn0.2Ni0.2Fe_2O_4 composites and its electrical-magnetic property. *J. Phys. Chem. C* **2010**, *114*, 6712−6717.

(26) Mao, H.; Lu, X.; Chao, D.; Cui, L.; Zhang, W. Controlled growth of poly (*N*-methylaniline): From nanowires to microspheres. *Mater. Lett.* **2008**, *62*, 998−1001.

(27) Jiang, J.; Yan, C.-S.; Liu, W. Facile template-free route to poly(*N*-methylaniline) microspheres in aqueous solution. *Mater. Lett.* **2009**, *63*, 2188−2190.

(28) Patil, R.; Sanada, K.; Jiang, X.; Harima, Y.; Masaoka, K.; Yamasaki, S.; Yano, J. Microspheres of conducting poly(*N*-methylaniline). *Polym. J.* **2004**, *36*, 549−555.

(29) Lü, Q.-F.; Huang, Z.-K.; Liu, B.; Cheng, X. Preparation and heavy-metal-ions biosorption of graft copolymers from enzymatic hydrolysis lignin and amino acids. *Bioresour. Technol.* **2012**, *104*, 111−118.

(30) Kriaa, A.; Hamdi, N.; Srasra, E. Removal of Cu (II) from water pollutant with Tunisian activated lignin prepared by phosphoric acid activation. *Desalination* **2010**, *250*, 179−187.

(31) Brdar, M.; Šćiban, M.; Takači, A.; Došenović, T. Comparison of two and three parameters adsorption isotherm for Cr(VI) onto Kraft lignin. *Chem. Eng. J.* **2012**, *183*, 108−111.

(32) Wu, Y.; Zhang, S.; Guo, X.; Huang, H. Adsorption of chromium(III) on lignin. *Bioresour. Technol.* **2008**, *99*, 7709−7715.

(33) Guo, X.; Zhang, S.; Shan, X.-Q. Adsorption of metal ions on lignin. *J. Hazard. Mater.* **2008**, *151*, 134−142.

(34) Adhikari, B. B.; Gurung, M.; Alam, S.; Tolnai, B.; Inoue, K. Kraft mill lignin − A potential source of bio-adsorbents for gold recovery from acidic chloride solution. *Chem. Eng. J.* **2013**, *231*, 190−197.

(35) Parajuli, D.; Adhikari, C. R.; Kuriyama, M.; Kawakita, H.; Ohto, K.; Inoue, K.; Funaoka, M. Selective recovery of gold by novel lignin-based adsorption gels. *Ind. Eng. Chem. Res.* **2006**, *45*, 8−14.

(36) Khunthai, K.; Parajuli, D.; Kawakita, H.; Inoue, K.; Funaoka, M. Adsorption behavior of quaternary amine types of lignophenol compounds for some precious metals. *Solvent Extr. Ion Exch.* **2010**, *28*, 393−414.

(37) Zhou, M.; Qiu, X.; Yang, D.; Lou, H.; Ouyang, X. High-performance dispersant of coal−water slurry synthesized from wheat straw alkali lignin. *Fuel Process. Technol.* **2007**, *88*, 375−382.

(38) Matsushita, Y.; Yasuda, S. Preparation and evaluation of lignosulfonates as a dispersant for gypsum paste from acid hydrolysis lignin. *Bioresour. Technol.* **2005**, *96*, 465−470.

(39) Lü, Q.-F.; Wang, C.; Cheng, X. One-step preparation of conductive polyaniline-lignosulfonate composite hollow nanospheres. *Microchim. Acta* **2010**, *169*, 233−239.

(40) Lü, Q.-F.; Zhang, J.-Y.; He, Z.-W. Controlled preparation and reactive silver-ion sorption of electrically conductive poly(*N*-butylaniline)−lignosulfonate composite nanospheres. *Chem. -Eur. J.* **2012**, *18*, 16571−16579.
(41) Lü, Q.-F.; Zhang, J.-Y.; Yang, J.; He, Z.-W.; Fang, C.-Q.; Lin, Q. Self-assembled poly(*N*-methylaniline)−lignosulfonate spheres: From silver-ion adsorbent to antimicrobial material. *Chem.—Eur. J.* **2013**, *19*, 10935−10944.
(42) Li, X. G.; Ma, X.-L.; Sun, J.; Huang, M. R. Powerful reactive sorption of silver(I) and mercury(II) onto poly(o-phenylenediamine) microparticles. *Langmuir* **2009**, *25*, 1675−1684.
(43) Li, X. G.; Huang, M. R.; Duan, W.; Yang, Y. L. Novel multifunctional polymers from aromatic diamines by oxidative polymerizations. *Chem. Rev.* **2002**, *102*, 2925−3030.
(44) Huang, M. R.; Lu, H.-J.; Li, X.-G. Synthesis and strong heavy-metal ion sorption of copolymer microparticles from phenylenediamine and its sulfonate. *J. Mater. Chem.* **2012**, *22*, 17685−17699.
(45) Huang, M. R.; Peng, Q.-Y.; Li, X.-G. Rapid and effective adsorption of lead ions on fine poly (phenylenediamine) microparticles. *Chem.—Eur. J.* **2006**, *12*, 4341−4350.
(46) Huang, M. R.; Huang, S.-J.; Li, X.-G. Facile synthesis of polysulfoaminoanthraquinone nanosorbents for rapid removal and ultrasensitive fluorescent detection of heavy metal ions. *J. Phys. Chem. C* **2011**, *115*, 5301−5315.
(47) Cui, H.; Qian, Y.; Qin, L.; Zhang, Q.; Zhai, J. Adsorption of aqueous Hg(II) by a polyaniline/attapulgite composite. *Chem. Eng. J.* **2012**, *211−212*, 216−223.
(48) Li, X.-G.; Feng, H.; Huang, M.-R. Strong adsorbability of mercury ions on aniline/sulfoanisidine copolymer nanosorbents. *Chem. -Eur. J.* **2009**, *15*, 4573−4581.
(49) He, Z.-W.; He, L.-H.; Yang, J.; Lü, Q.-F. Removal and recovery of Au(III) from aqueous solution using a low-cost lignin-based biosorbent. *Ind. Eng. Chem. Res.* **2013**, *52*, 4103−4108.
(50) Olad, A.; Nabavi, R. Application of polyaniline for the reduction of toxic Cr(VI) in water. *J. Hazard. Mater.* **2007**, *147*, 845−851.
(51) Gu, H.; Rapole, S. B.; Sharma, J.; Huang, Y.; Cao, D.; Colorado, H. A.; Luo, Z.; Haldolaarachchige, N.; Young, D. P.; Walters, B.; Wei, S.; Guo, Z. Magnetic polyaniline nanocomposites toward toxic hexavalent chromium removal. *RSC Adv.* **2012**, *2*, 11007−11018.
(52) Ameen, S.; Akhtar, M. S.; Shin, H. S. A sea-cucumber-like hollow polyaniline spheres electrode-based chemical sensor for the efficient detection of aliphatic alcohols. *RSC Adv.* **2013**, *3*, 10460−10470.
(53) Lu, X.; Zheng, J.; Chao, D.; Chen, J.; Zhang, W.; Wei, Y. Poly (*N*-methylaniline)/multi-walled carbon nanotube composites—Synthesis, characterization, and electrical properties. *J. Appl. Polym. Sci.* **2006**, *100*, 2356−2361.
(54) Kadla, J. F.; Kubo, S. Lignin-based polymer blends: Analysis of intermolecular interactions in lignin−synthetic polymer blends. *Compos. Part A-Appl. S.* **2004**, *35*, 395−400.
(55) Lu, X.; heng, J.; Chao, D.; Chen, J.; Zhang, W.; Wei, Y. Poly (*N*-methylaniline)/multi-walled carbon nanotube composites—Synthesis, characterization, and electrical properties. *J. Appl. Polym. Sci.* **2006**, *100*, 2356−2361.
(56) Guerra, A.; Mendonc, R.; Ferraz, A.; Lu, F.; Ralph, J. Structural characterization of lignin during *Pinus taeda* wood treatment with *Ceriporiopsis subvermispora*. *Appl. Environ. Microb.* **2004**, *70*, 4073−4078.
(57) Li, X.-G.; Liu, R.; Huang, M.-R. Facile synthesis and highly reactive silver ion adsorption of novel microparticles of sulfodiphenylamine and diaminonaphthalene copolymers. *Chem. Mater.* **2005**, *17*, 5411−5419.
(58) Abthagir, P. S.; Saraswathi, R.; Sivakolunthu, S. Aging and thermal degradation of poly(*N*-methylaniline). *Thermochim. Acta* **2004**, *411*, 109−123.
(59) Harima, Y.; Sanada, K.; Patil, R.; Ooyama, Y.; Mizota, H.; Yano, J. Monodisperse and isolated microspheres of poly(*N*-methylaniline) prepared by dispersion polymerization. *Eur. Polym. J.* **2010**, *46*, 1480−1487.
(60) Khan, S. A.; Rehman, R.; Khan, M. A.. Adsorption of chromium (III), chromium (VI) and silver (I) on bentonite. *Waste Manage.* **1995**, *15*, 271−282.
(61) Homan, K. A.; Chen, J.; Schiano, A.; Mohamed, M.; Willets, K. A.; Murugesan, S.; Stevenson, K. J.; Emelianov, S. Silver−polymer composite stars: Synthesis and applications. *Adv. Funct. Mater.* **2011**, *21*, 1673−1680.
(62) Dong, X.; Dong, M.; Lu, Y.; Turley, A.; Jin, T.; Wu, C. Antimicrobial and antioxidant activities of lignin from residue of corn stover to ethanol production. *Ind. Crop. Prod.* **2011**, *34*, 1629−1634.
(63) Dizhbite, T.; Telysheva, G.; Jurkjane, V.; Viesturs, U. Characterization of the radical scavenging activity of lignins−−natural antioxidants. *Bioresour. Technol.* **2004**, *95*, 309−317.